Available online at www.sciencedirect.com

ScienceDirect

journal homepage: www.elsevier.com/locate/jtte

Original Research Paper

Study of the influence of pavement unevenness on the mechanical response of asphalt pavement by means of the finite element method

Pengfei Liu [a], *Visaagan Ravee* [a], *Dawei Wang* [a,b,*], *Markus Oeser* [a]

[a] *Institute of Highway Engineering, RWTH Aachen University, Aachen 52074, Germany*
[b] *School of Transportation Science and Engineering, Harbin Institute of Technology, Harbin 150090, China*

HIGHLIGHTS

- Tire-pavement interaction FE models are developed.
- The model is verified by means of analytical and experimental methods.
- The results from uneven pavements are compared with flat pavements.

ARTICLE INFO

Article history:
Received 9 October 2017
Received in revised form
21 December 2017
Accepted 22 December 2017
Available online 14 June 2018

Keywords:
Pavement
Unevenness
Mechanics
Finite element method (FEM)
Interaction

ABSTRACT

Pavement unevenness affects the vehicle operating cost, speed, riding comfort, safety, pavement service life and etc. The current mechanistic-empirical (M-E) design procedure of asphalt pavements is based on the computational model of a flat pavement instead of uneven pavement as it is the case in reality. In this paper, a tire-pavement-interaction FE model is developed to investigate the influence of pavement unevenness on the mechanical responses of asphalt pavements. For both winter and summer conditions, the strain at the bottom of the asphalt layer due to the tire load is found to decrease as the wavelength of the unevenness increases. Moreover, the strain is larger at lower speeds and decreases as the speed increases. It is found that the stress levels are higher in summer conditions than under winter conditions for the same pavement irrespective of wavelength. The fatigue life increases with increase in speed of the tire for a pavement and also increases with increase in the wavelength of the pavement unevenness. The results indicate that pavement unevenness significantly influence the mechanical responses of asphalt pavements and thus influences the service life of asphalt pavements. As a result, the current M-E design algorithm of asphalt pavements should be modified to consider the pavement unevenness to allow better design processes for asphalt pavement.

* Corresponding author. Institute of Highway Engineering, RWTH Aachen University, Aachen, 52074, Germany. Tel.: +86 451 86283090; fax: +86 451 86283090.
E-mail addresses: liu@isac.rwth-aachen.de (P. Liu), visaagan.ravee@rwth-aachen.de (V. Ravee), wang@isac.rwth-aachen.de (D. Wang), oeser@isac.rwth-aachen.de (M. Oeser).
Peer review under responsibility of Periodical Offices of Chang'an University.
https://doi.org/10.1016/j.jtte.2017.12.001

1. Introduction

Pavement unevenness affects the vehicle operating cost, speed, riding comfort, safety, fuel consumption, wear of tires, and pavement service life (Zhang et al., 2017). The occurrence of pavement unevenness as seen in Fig. 1 is influenced by the applied construction technology (including processes and equipment), the state of compaction, the construction quality control, the structure of the surface course and the materials (e.g., binder, aggregate and air voids), etc (Liu et al., 2017a,b; Hu et al., 2016; Wang et al., 2017a,b).

Pavement unevenness can lead to dynamic loads being induced on pavements; thus, the mechanical responses of uneven pavements will be significantly different with those of flat pavements (Ueckermann et al., 2015; Ueckermann and Steinauer, 2008). The current mechanistic-empirical (M-E) design procedure for asphalt pavements is based on the computational model of flat pavements (Gonzalez and Oeser, 2012). This idealization results in discrepancies from reality. Therefore, the influence of pavement unevenness on the mechanical responses of asphalt pavements needs to be studied. The finite element method (FEM) is an effective tool to study the mechanical response of asphalt pavements (Zienkiewicz and Taylor, 2000, 2005), and the tire-pavement interaction which has been used in past years (Liu et al., 2013, 2014; 2017c; Oeser and Möller, 2002).

Liu et al. (2017d) investigated the impact of heavy traffic loads on the asphalt pavement in terms of stress and strain distribution, surface deflection and fatigue life by using FEM code. In this FEM code, the tire can be implicitly simulated by an algorithm which simulates the movement process of the wheel realistically (Liu et al., 2015). The vertical pressure was distributed over a square contact area including several elements and the load process was divided into several increments. In such an increment when the mass center of wheel was exactly above the contact area, the elements covered by the contact area were assumed to be fully loaded. In subsequent increments the elements behind the wheel would be partly relieved and the elements in front of the wheel would be partly loaded. With this procedure, the load distribution of a rolling wheel approximated. Kaliske et al. (2015), Wollny and Kaliske (2013) and Wollny et al. (2016a,b) proposed a theoretical-numerical asphalt pavement model at material and structural level, whereby the focus is on a realistic and numerically efficient computation of pavements under a rolling tire load by using FEM based on an arbitrary Lagrangian Eulerian (ALE) formulation. In the ALE frame, the pavement was described in a moved reference configuration, so that the loading of the pavement with a rolling tire could be described as a time-independent process. Pavement structures under the load of a rolling truck tire were simulated. Stresses, strains and displacements of the pavement structures as well as the effect of different driving velocities of the tire were evaluated (Zopf et al., 2015). Wang et al. (2012) constructed a three-dimensional (3D) tire-pavement interaction model in the general-purpose FE program ABAQUS to predict the contact stress distributions for future use in the mechanistic analysis of pavement responses. A ribbed radial-ply tire was modeled as a composite structure (rubber and reinforcement); the tire material parameters were calibrated through load-deflection curves. The tire rolling process was also simulated using an ALE formulation. The model results were consistent with previous measurements and validated the existence of non-uniform vertical contact stresses and localized tangential contact stresses. The analysis results showed that the non-uniformity of vertical contact stresses decreased as the load increased, but increased as the inflation pressure increased. Vehicle maneuvering is affected significantly by the tire-pavement contact stress distributions.

However, few previous investigations focused on the influence of the pavement unevenness on the mechanical response of asphalt pavements. In this study, the tire-pavement interaction FE models with different situations of pavement unevenness are developed. The modeling algorithm is described in detail. Verification of the developed FE model is carried out by means of analytical and experimental methods. Using this reliable FE model, the influence of the pavement unevenness on the mechanical response of asphalt pavements is studied.

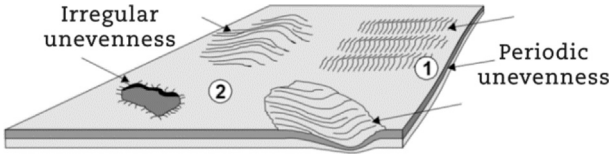

Fig. 1 – Periodic and irregular unevenness in the longitudinal direction (Krause and Maerschalk, 2010).

Table 1 – Selected tire specifications.

Feature	Value
Overall diameter of the tire (mm)	970.0
Diameter of the rim (mm)	571.5
Section width of the tire (mm)	295.0
Thread depth (mm)	15.0
Max load capacity (kN)	26.7

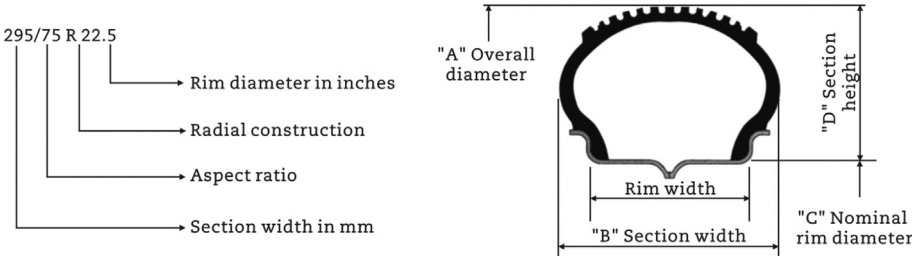

Fig. 2 – Tire specification (Panhead and Flathead Documentation, 2017).

2. FE simulation of pavement responses

2.1. Development of the FE model

2.1.1. Development of the tire model

In order to derive mechanical response of asphalt pavement under heavy traffic loading, a truck tire 295/75R22.5 from Continental was selected (Continental, 2017). The specification of the tire and its geometry are shown in Fig. 2 and Table 1.

Since this study focuses on the mechanical response of the asphalt pavement, the tire model is simplified with a detailed thread, a body section (neglecting the belt and cord) and a rim. In order to improve the computational efficiency, the thread and body section of the tire are considered as elastic. The rim is taken into consideration as rigid body. The material properties from the previous work from Dassault Systèmes Simulia Corp (Lin and Hwang, 2004) are utilized for the tire, which is listed in Table 2.

Table 2 – Material properties of the tire.

Material parameter	Thread and body section	Rim
Density (kg/m^3)	719	8000
Poisson's ratio	0.3	0.3
Young's modulus (MPa)	80	200,000

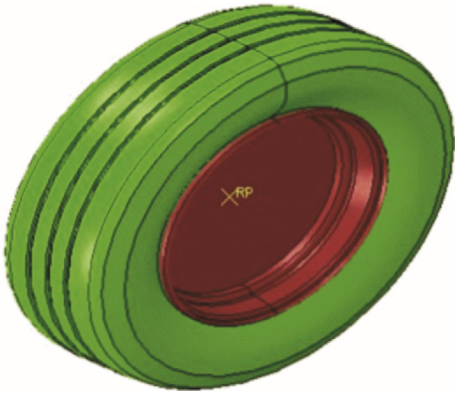

Fig. 3 – 3D tire model.

The 3D model of the tire is based on the two-dimensional (2D) cross section of the 295/75R22.5 tire, as shown in Fig. 3. The rim is tied to a reference point which lies on the axis of rotation of the tire. This reference point is helpful in applying perpendicular loads to the pavement and providing the angular rotation boundary condition for the tire. 39,108 solid elements (type C3D8R) are utilized to discretize the thread and body section; the total number of nodes is 73,635.

2.1.2. Development of the pavement model

Different types of FE pavement models were developed in different dimensions for different simulations throughout this study. One model (5.00 m × 0.80 m × 0.04 m) is used for the tire model verification, and a second model (3.75 m × 3.75 m × 2.92 m) is used for pavement verification, and the third model with different dimensions is used for the simulation of pavement unevenness, as shown in Fig. 4. The element size in close proximity to the tire-pavement contact area is made smaller than the global element size. More details regarding the geometry and material properties of the pavement models are explained in the following sections.

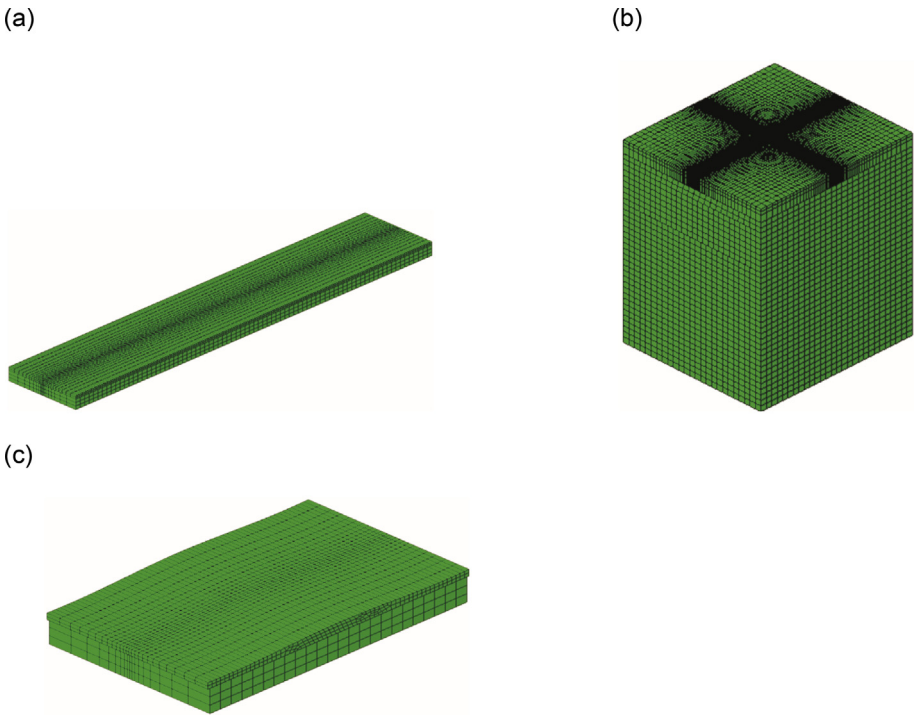

Fig. 4 – Different types of pavement models. (a) Pavement model used for the tire model verification. (b) Pavement model used for pavement verification. (c) Pavement model used for the simulation of pavement unevenness.

2.1.3. *Development of the tire-pavement interaction model*

In this study, the tire-pavement interaction simulation is carried out in three steps: tire inflation, tire loading on to the pavement and the tire movement along the pavement. The entire simulations are carried out in ABAQUS/Explicit.

In the tire inflation step, the center of the tire is fixed and an inflation pressure of 0.759 MPa is applied on the inner surface of the tire. The tire is maintained at a distance from the pavement surface without contact. The entire tire inflation step is assigned with a time of 4 s. As shown in Fig. 5 the black lines represent the tire contour before the inflation step and the colored image represent the tire contour after inflation.

Fig. 6 depicts the state of the simulation before the loading step is initiated. The gap between the tire and the top surface of the pavement can be seen clearly. In the tire loading simulation, the tire is moved on towards the pavement. The tire loading is done by applying gravitational force and axle loads on the reference point of the tire and bringing the tire into contact with the pavement.

In order to stabilize the tire before the rotation step, the simulation time of the loading step is set as 10 s. Fig. 7 shows the displacement evolution of the reference point of the tire over the simulation time. When the loading step is carried out longer than 10 s, the results clearly shows that the tire comes to a rest.

At the end of the loading step the tire comes in contact stably with the pavement leading to a deformation in the tire due to the contact pressure. Fig. 8 indicates the effect of tire loading on stress distribution of the tire and contact area on the pavement.

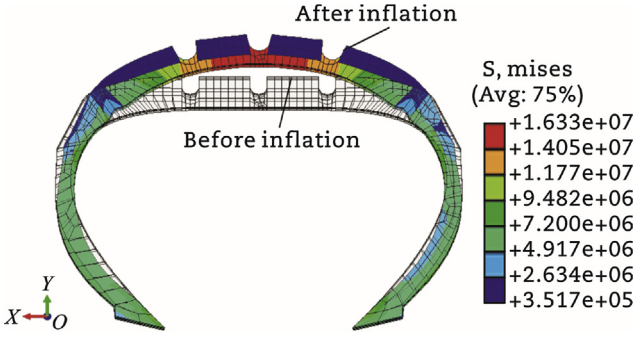

Fig. 5 – Deformation of the tire models during inflation step.

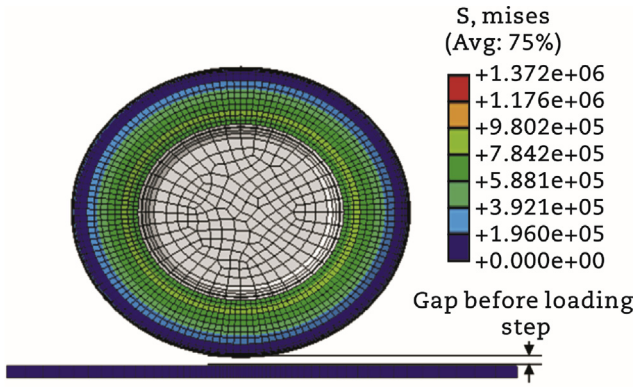

Fig. 6 – Tire-pavement before initiation of the loading step.

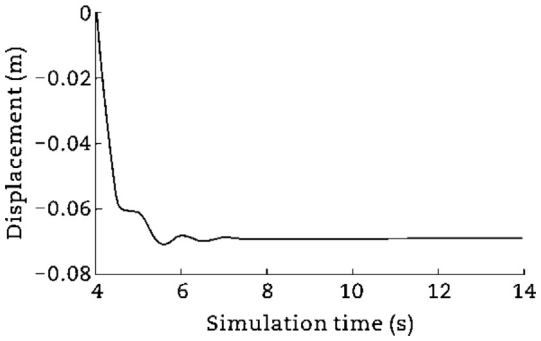

Fig. 7 – Displacement evolution of reference point of tire with simulation time.

In the tire rotation step, a constant angular velocity is defined based on the reference point of the tire. The defined general contact interaction property in ABAQUS for the tire-pavement contact with a friction coefficient of 0.3 helps to convert the constant rotation of the tire into a longitudinal movement along the pavement (ABAQUS, 2011). Fig. 9 shows the tire rotation in the third step of the simulation. The tire rotation time is selected based on the speed and the length of the pavement.

The linear velocity is converted in to angular velocity by the following equation

$$\omega = \frac{v}{r} \tag{1}$$

where ω is the angular velocity, v is the linear velocity, r is the radius of the tire. The radius of the tire is 0.49 m and the different velocities used in this study are shown in Table 3.

2.2. *Verification of the FE model*

2.2.1. *Analytical verification of the tire-pavement interaction model*

In order to verify the tire-pavement interaction model, a simulation was carried out first, in which the tire rolled over a ditch profile with edges perpendicular to the direction of travel at a speed of 19.3 km/h. The vertical displacement of the tire spindle is compared with the results from literature (Chae, 2006).

The ditch profile used for determining the dynamic tire responses is a 690 mm long and 120 mm deep water drainage ditch as shown in Fig. 10. The radius of curvature is 0.78 m. The pavement and ditch are modeled with a rigid material.

The only difference between the developed tire model and studies found in literature (Chae, 2006) is the simplified tire material model used in this study. Fig. 11 compares the vertical displacement of the tire spindle obtained from the developed tire model and data from literature (Chae, 2006). The results show that the developed model exhibits reasonable vertical displacement responses of the tire spindle.

2.2.2. *Experimental verification of the tire-pavement interaction model*

The tire-pavement interaction model was then verified with data derived from measurements on the test track of German

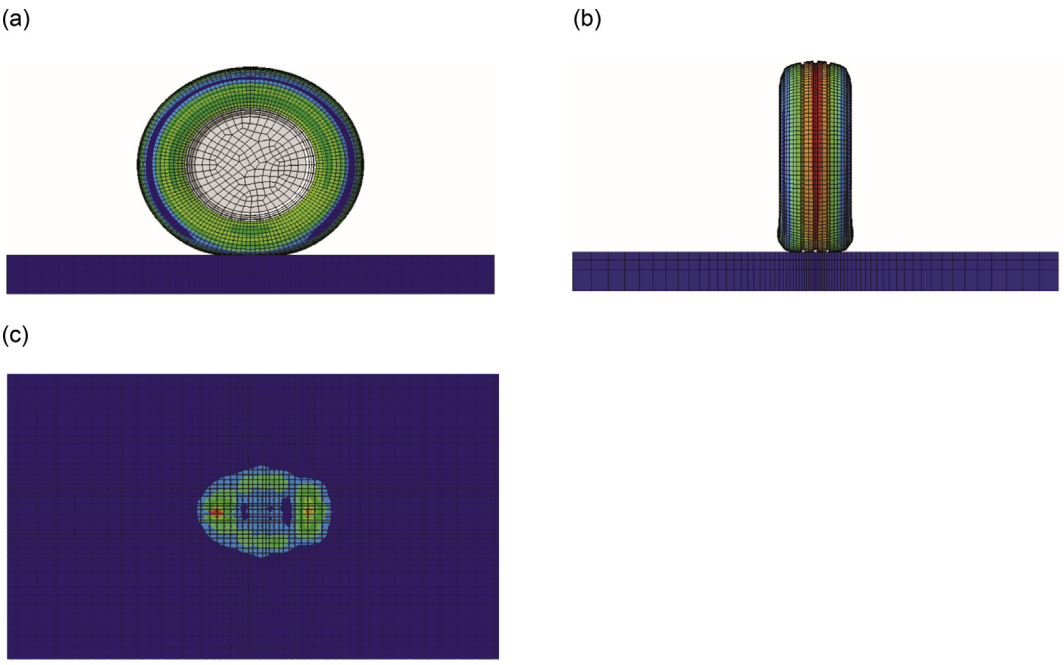

Fig. 8 – Stress in tire loading and tire deformation. (a) Side view of the tire-pavement model. (b) Front view of the tire-pavement model. (c) Top view of the pavement model.

Federal Highway Research Institute (BASt), as shown in Fig. 12. During the test track construction, strain gauges and pressure load cells were embedded at different depths, which can measure strains and stresses along corresponding directions when loads are applied (Liu et al., 2016, 2017b).

According to the suggestion by Gohl (2006) and Rabe (2004, 2007, 2014), a dynamic analysis with a tire speed of 30 km/h was carried out in this study. The geometry and material properties of the pavement are displayed in Table 4. The length and the width of the pavement were set to 3750 mm.

The 3D tire-pavement interaction was modeled in ABAQUS and shown in Fig. 13. The pavement model is developed with 8-node linear brick elements (C3D8R) and a fine mesh in close proximity to the contact area and a relatively coarse mesh elsewhere. The boundary conditions and the interaction properties between the layers vary between the layers.

All sides of the pavement are set with symmetrical boundary conditions so that the size of the pavement has a minimum effect on the results. The bottom of the sub-grade layer is fixed in all directions. The top three asphalt courses are fully bound together. The interfaces between road base course, sub-base and the sub-grade are partially bound, which only allows relative displacement in horizontal directions at the interlayers.

The strain at the bottom of the asphalt base course and the stress at top of the road base course are taken as the measure for verification. The values from the simulation are compared with the measurement, as shown in Table 5. Due to

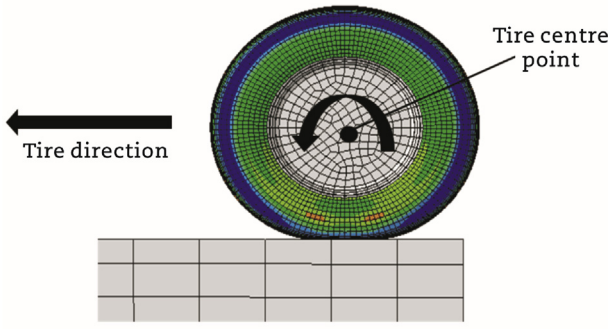

Fig. 9 – Process of tire rotation.

Table 3 – Different linear and angular velocities used in this study.

Speed (km/h)	Linear velocity (m/s)	Angular velocity (rad/s)
19.3	5.36	10.94
30.0	8.33	17.00
50.0	13.89	28.35
70.0	19.44	39.67

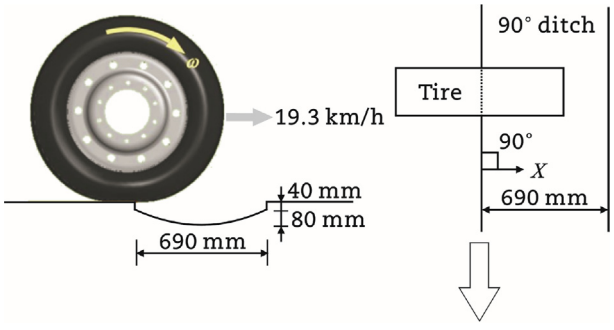

Fig. 10 – Water drainage ditch profile (Chae, 2006).

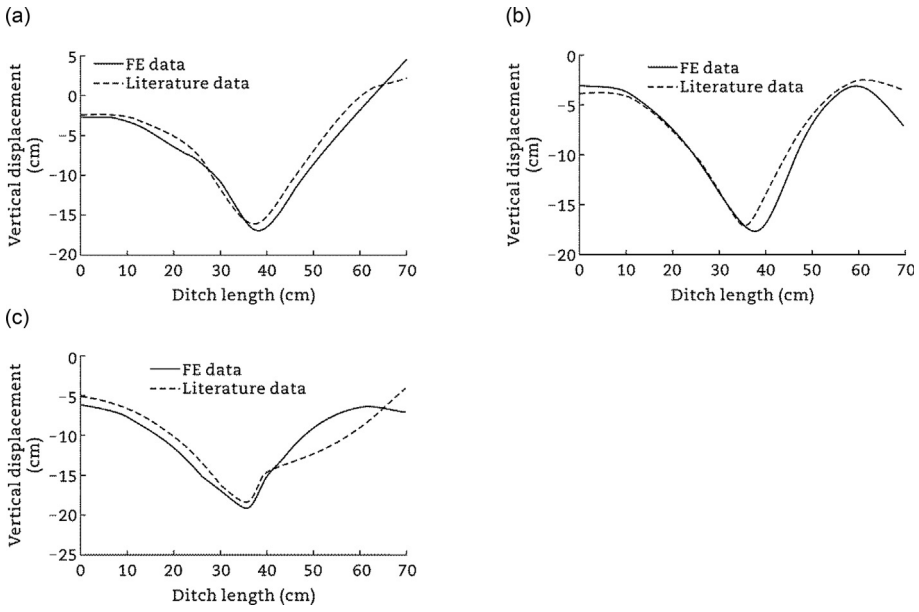

Fig. 11 – Comparison between vertical displacements of the tire spindle for loads of different ditch lengths that derived from this study and literature (a) 13.3 kN (b) 26.7 kN (c) 40 kN (Chae, 2006).

Fig. 12 – Test track facility at BASt (Gohl, 2006).

Table 4 – Geometrical data and material properties of the pavement.

Layer	Thickness (mm)	E (MPa)	μ	Density (t/mm^3)
Surface course	40	11,150.0	0.35	2.377×10^9
Binder course	50	10,435.0	0.35	2.448×10^9
Asphalt base course	110	6893.0	0.35	2.301×10^9
Road base course	150	157.8	0.49	2.400×10^9
Sub-base	570	125.7	0.49	2.400×10^9
Sub-grade	2000	98.9	0.49	2.400×10^9

uncertainties and fluctuations, the error range is considered to be 20% (Liu et al., 2017c). The relative errors between the results from the simulation and measurement are −12% and −3.6%, respectively, which is in the error range. The interaction model is verified based on the abovementioned criteria and utilized for the further simulations with uneven pavement surfaces.

2.3. *Uneven asphalt surface pavement modeling*

The developed tire-pavement interaction model was utilized to study the effect of pavement unevenness. A simplified two-layered pavement was constructed according to a previous study to reduce the computational efforts (Liu et al., 2016, 2017b). The top layer is an asphalt layer and the bottom is a road base layer. To investigate the mechanical response of asphalt pavement the pavement evenness was varied in the simulations. The longitudinal profile of the pavement was assumed to be a sinusoidal function. According to the wavelength range of the pavement evenness proposed by Yao (2006) and the kinematic model proposed by Song (2005) and ISO 2631–1:1997(e) it is suitable for the simulation of vehicles driving on pavements with a wave-like shape, as shown in Fig. 14.

In Fig. 14 *a*, *b*, *c*, and *d* represent the wavelength, amplitude, thickness of asphalt layer and thickness of the bottom layer respectively. The appropriate wavelength and amplitude were selected. The selection was based on the balance of the computational efficiency and research purpose. These parameters are given in Table 6.

Different simulations are carried out with varying unevenness wavelengths whilst maintaining a constant amplitude in the vertical direction. For each wavelength, multiple simulations are carried out varying the wheel speed and the pavement properties for summer and winter conditions. The material and geometric data of the pavement layers are shown in Table 7 (Liu et al., 2016).

The length of the pavement is determined according to the wavelength of the unevenness. For example, if the wavelength is 15 m then the length of the pavement is set to be 30 m

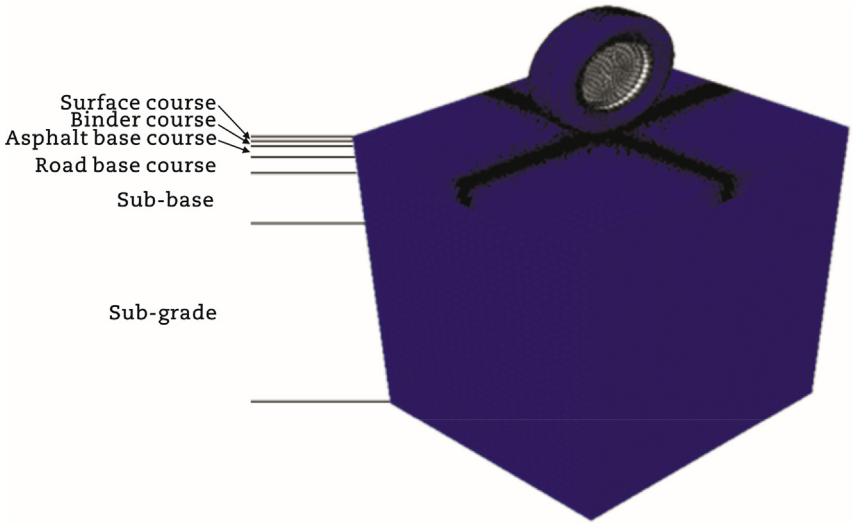

Fig. 13 – ABAQUS generated mesh model of a pavement with 6 layers.

Table 5 – Comparison of measured stress and strain results with the FE results.

	Measurement	Simulation	Relative error (%)
Strain at bottom of asphalt base course (μm/m)	80	70	−12
Stress at top of road base course (MPa)	0.055	0.053	−3.6

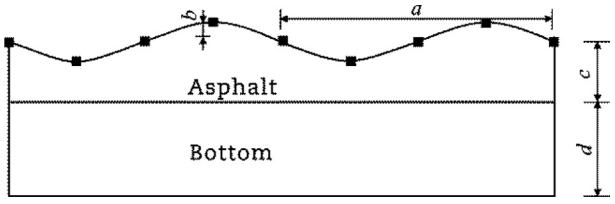

Fig. 14 – Uneven pavement surface model parameters.

Table 6 – Pavement evenness parameters of simulation test scene.

Wavelength (m)	Amplitude (cm)	Speed (km/h)
45	5	30, 50 and 70
30	5	30, 50 and 70
15	5	30, 50 and 70
5	5	30, 50 and 70

Table 7 – Material properties of the uneven pavement.

Layer	E (MPa)		μ	Density (t/mm^3)
	Winter	Summer		
Asphalt	21,500	5200	0.30	2.356×10^9
Road base	135	135	0.49	2.400×10^9

to ensure that at least two waves are contained. In the two-layered pavement model the two most important boundary conditions to be considered are the interaction between the pavement layers and the encastre boundary condition at bottom of the model. The interaction properties between the pavement layers are selected that the pavement layers are not restricted in the horizontal direction, while the pavement layers are bound in the vertical direction.

The 295/75R22.5 tire is used for the simulations on the uneven asphalt pavement surface. The simulations involve three different steps, which were already described in section 2.1.3. In total, 30 simulations are carried out in this study, including simulations of a flat pavement. The model is shown in Fig. 15.

3. Results and discussions

3.1. *Visualization of stress state*

To study the distribution of the stress state and deformation in the pavements, cross-sections are made along the direction

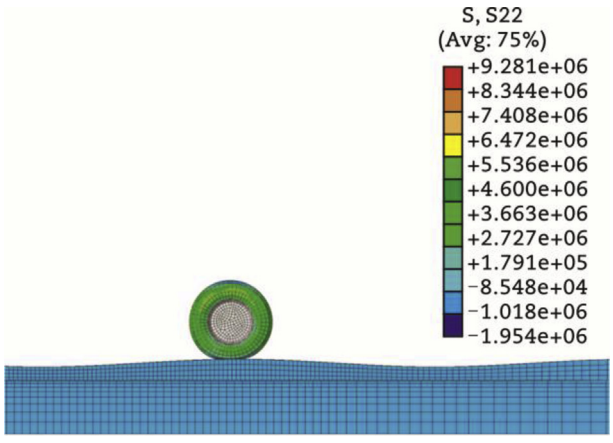

Fig. 15 – Model of uneven pavement.

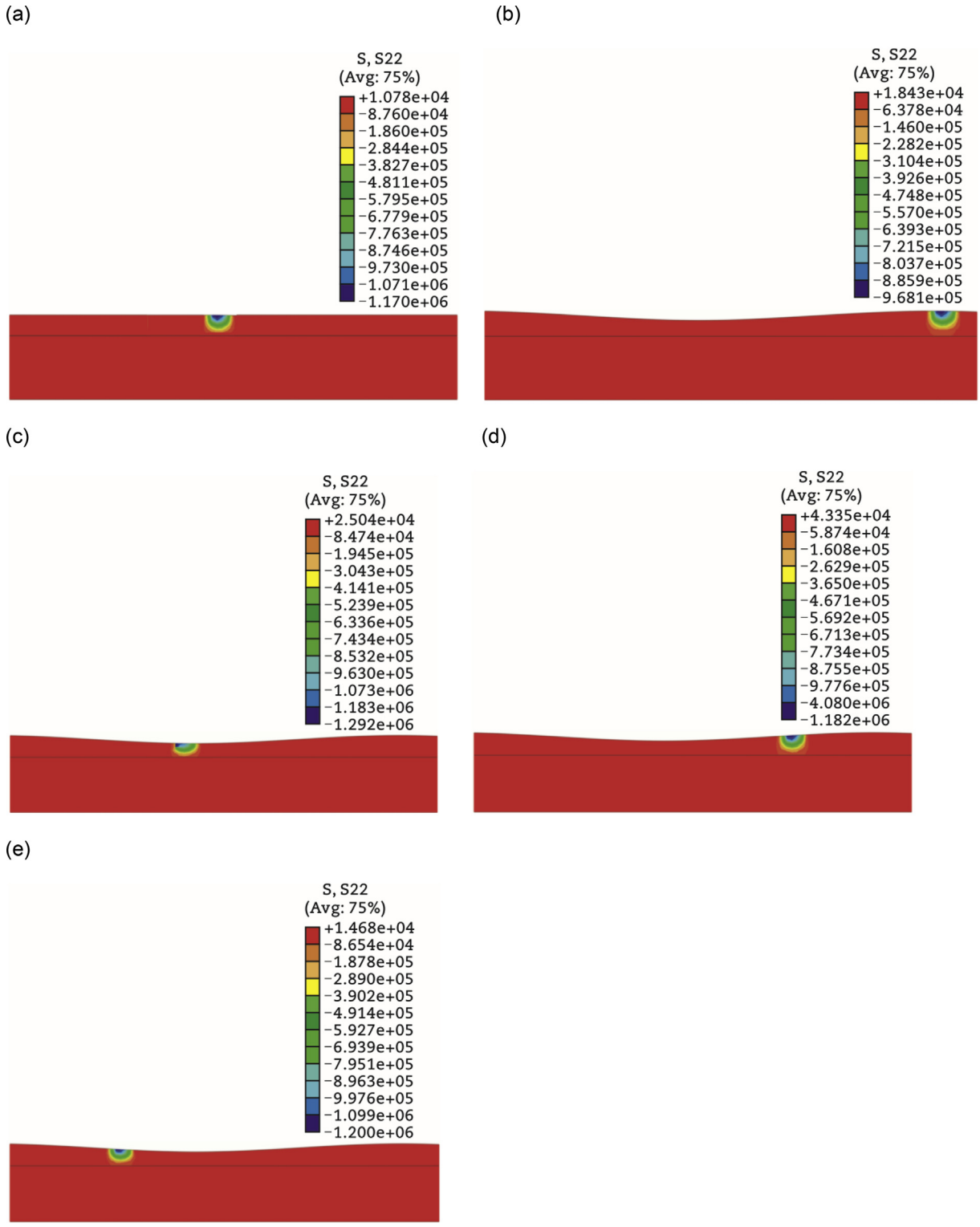

Fig. 16 – The distribution of vertical stress (Pa) in the pavement with the tire speed of 30 km/h in the summer. (a) At the surface of flat pavement. (b) At the crest of the pavement with wavelength of 5 m. (c) At the trough of the pavement with wavelength of 5 m. (d) At the mid-location from crest to trough of the pavement with wavelength of 5 m. (e) At the mid-location from trough to crest of the pavement with wavelength of 5 m.

of travel. A flat pavement model and a tire moving with the speed of 30 km/h is selected as a reference and compared to a pavement model with a 5 m wavelength. Material properties under summer conditions were used. The vertical stresses are evaluated when the tire is on the crest, trough and at the two locations between crest and trough and the locations are visualized in Fig. 16. Large vertical stress occurs close to the loading area and decreases rapidly with the increase of distance from the loading area. It is highly important to investigate the near-surface pavement response due to the great deformation in this region. Moreover, the largest stresses occur when the tire is on the trough which is followed by those the tires are at the mid-locations. The vertical stress when the tire is on the crest is the smallest. The rank order of results is the same for all pavement models and all speeds.

3.2. *Effect of pavement unevenness on mechanical response of asphalt pavement*

3.2.1. *Effect of wavelength and speed on mechanical response of uneven pavement*

To study the effect of the unevenness, the strain at the bottom of the asphalt layer and the stress at top of the base layer are analyzed. Comparisons are made between the results derived from the trough of the second wave in all the uneven pavement models, which has been shown to be the critical stress state with stable results. As a reference, the results of the flat pavement model are also taken into consideration for the comparison.

The strains at bottom of the asphalt layer under summer conditions are plotted in Fig. 17. The strain values of the flat pavement are the smallest for all simulations. The strain decreases as the wavelength of the unevenness increase, i.e., the 5 m wavelength pavement model has the highest strain at the bottom of the asphalt layer for every speed while the 45 m wavelength exhibits the lowest strain, closest to the strain from a flat pavement. Moreover, the strain is larger at lower speed and decreases as the speed increases.

The maximum stresses at the top of the base layer for different wavelengths and speed under summer conditions are shown in Fig. 18.

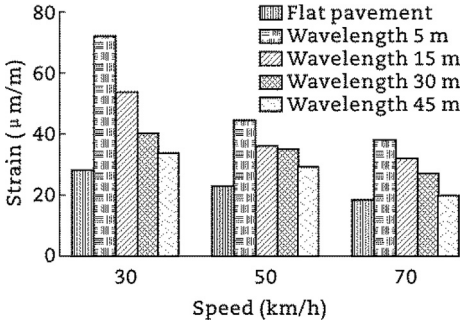

Fig. 17 – Comparison of the horizontal strain along the transverse traffic direction at the bottom of the asphalt layer in summer.

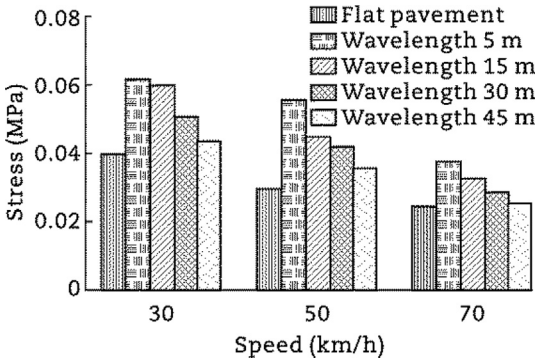

Fig. 18 – Comparison of the vertical stress at the top of the base layer under summer conditions.

The stress values at the top of the base layer are listed in Table 8. The values of the flat pavement are the lowest while the stress values decrease as the wavelength of the unevenness increases. When the ratio of the wavelength to the amplitude increases, the stress at the top of the base layer decreases. Furthermore, a speed of 30 km/h exhibits the highest stress at the top of the base layer for all pavement models. As the speed increases, the stress at the top of the base layer decreases. The same trend is also found in the results derived from the simulations for pavements under winter conditions. An analysis of the effect of seasonal conditions will be conducted later, therefore, the results under winter conditions are not described here.

3.2.2. *Effect of seasonal conditions on the mechanical response of uneven pavements*

From the different simulations under summer and winter conditions the effect of weather on the stress and strain at the pavement layers can be analyzed. The materials exhibit different elastic moduli depending on the seasonal conditions which result in altered stress and strain states. Fig. 19 shows the comparison of the vertical stress at the top of the base layer at different speeds for both summer and winter conditions (unevenness wavelength of 5 m). As seen in Fig. 19 the winter conditions exhibit smaller stresses compared to summer conditions due to the higher elastic modulus.

Similarly, the vertical stress at the top of the base layer are compared for different wavelengths in Fig. 20. The speed of the wheel is set constant at 30 km/h for this comparison. It is evident that the seasonal variations follow the same trend irrespective of unevenness wavelengths; the stress results are higher under summer conditions and lower under winter conditions.

3.3. *Predicting the fatigue life of the asphalt pavement*

The fatigue life of the asphalt pavement can be calculated according to Eq. (2), which is derived from indirect tensile tests on drill cores extracted from the asphalt base layers according to German rules and regulations (FGSV, 2009):

$$N_{\text{insitu}} = 2.8283 N_f \varepsilon^{-4.194} \quad (2)$$

Table 8 – Stresses at the top of the base layer for different pavement under summer conditions (MPa).

Speed (km/h)	Flat pavement	Wavelength (m)			
		5	15	30	45
30	3.99e-02	6.17e-02	5.98e-02	5.07e-02	4.34e-02
50	2.95e-02	5.52e-02	4.45e-02	4.22e-02	3.55e-02
70	2.42e-02	3.72e-02	3.25e-02	2.85e-02	2.55e-02

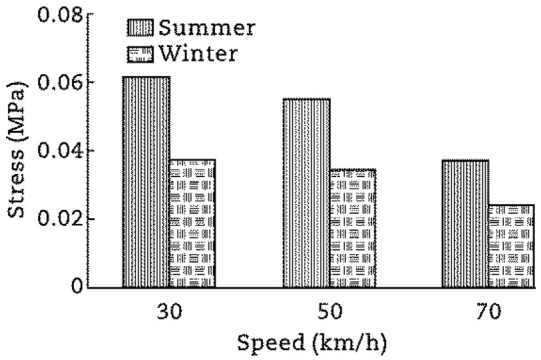

Fig. 19 – Comparison of the vertical stress at the top of the base layer for summer and winter conditions (unevenness wavelength of 5 m).

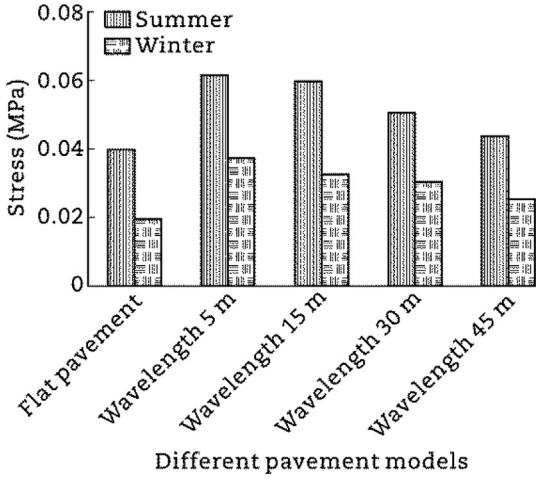

Fig. 20 – Comparison of the vertical stress at the top of the base layer for summer and winter conditions at a constant speed of 30 km/h.

where N_{insitu} is the number of load cycles until macro crack initiation is observed, N_f is the shift factor, in this case N_f is 1540 (Gohl, 2006), ε is the computational tensile strain at the bottom of the asphalt layer.

The tensile strain and fatigue life of the different asphalt layers under summer conditions are listed in Table 9 for varying wheel speed. The fatigue life increases as the speed increases, i.e., an increase in the speed reduces the reaction time for a single point on the pavement thereby reducing the strain – this ultimately increases the life of the asphalt pavement. Similarly, the fatigue life increases with an increase of the wavelength of the unevenness in the pavement, i.e. the shorter wavelengths (up to 5 m in this study) result in a more rapid deterioration of the pavement. Based on the conducted simulations, it is evident that a pavement with an unevenness wavelength of 45 m exhibits fatigue life similar to that of a flat pavement. Further increasing the wavelength of unevenness will approach the values of a flat pavement.

Table 9 – Tensile strain and fatigue life of different asphalt layers under summer conditions.

Pavement model	Speed (km/h)	Tensile strain (μm/m)	Fatigue life (10^{22})
Flat pavement	30	28.1	5.30
	50	23.2	11.91
	70	18.2	32.98
Wavelength 5 m	30	72.6	0.09
	50	44.6	0.77
	70	38.1	1.48
Wavelength 15 m	30	54.0	0.34
	50	35.9	1.90
	70	32.1	3.05
Wavelength 30 m	30	40.6	1.13
	50	35.2	2.07
	70	27.1	6.21
Wavelength 45 m	30	33.5	2.55
	50	28.9	4.74
	70	20.1	21.74

The strains under winter conditions at different speeds are listed in Table 10 including the fatigue life of the asphalt pavements for winter conditions. Similar trends are found as under summer conditions. Given the same experimental

Table 10 – Tensile strain and fatigue life of different asphalt layers under winter conditions.

Pavement model	Speed (km/h)	Tensile strain (μm/m)	Fatigue life (10^{22})
Flat pavement	30	20.9	18.46
	50	18.6	30.10
	70	12.5	159.40
Wavelength 5 m	30	28.3	5.17
	50	24.7	9.16
	70	23.7	10.89
Wavelength 15 m	30	28.1	5.33
	50	20.5	18.66
	70	15.2	70.20
Wavelength 30 m	30	25.6	7.88
	50	20.3	18.92
	70	14.9	71.30
Wavelength 45 m	30	24.6	9.80
	50	20.1	19.22
	70	14.4	88.07

design, the fatigue life of the pavement under winter conditions is much longer than under summer conditions.

4. Summary

In this paper a tire-pavement-interaction FE model is developed to investigate the influence of pavement unevenness on the mechanical responses of asphalt pavements. The FE model is verified with analytical and experimental data. The uneven pavement models with different wavelengths and amplitudes are created and evaluated for summer and winter conditions; the results are compared with those of a flat pavement surface based on the critical stress, strain and fatigue life.

The following results are derived from the FE simulation. For both winter and summer conditions, the strain at the bottom of the asphalt layer decreases as the wavelength of the unevenness increases, i.e., the 5 m unevenness-wavelength exhibits the highest strain at the bottom of the asphalt layer for speed whilst the 45 m unevenness-wavelength exhibits the lowest strain, very close to the strain observed for a flat pavement. Moreover, the strain is larger at lower speeds and decreases as the speed increases. The stress values at the top of the base layer show the same trend as for the strains. The different seasonal conditions result in different elastic moduli of the pavement materials and therefore the pavements show different stress and strain responses. The stress results are higher for summer conditions and lower for winter conditions irrespective of the unevenness-wavelength (or flat pavement). The fatigue life of asphalt pavements increases as the speed increases and also increases as the unevenness-wavelength increase. The results indicate that the influence of pavement unevenness significantly influences the mechanical responses of asphalt pavements and thus influences the service life of asphalt pavements. As a result, the current M-E design algorithm of asphalt pavements should consider the pavement unevenness to better design asphalt pavements.

As an initial research on this field, much future work is required. A tire model with higher complexity with inner components may be implemented. Due to computational requirements, a small pavement model was used. Longer pavement models may result in more stable results. An improvement of methodology could be achieved by implementing smaller meshing at the tire contact regions. Further methods to improve the simulation time with ABAQUS can also be explored. Also, a more realistic longitudinal unevenness of the pavement surface can be taken into consideration.

Acknowledgments

This paper is part of the research project carried out at the request of the German Research Foundation (DFG), under research project OE 514/1–2 (FOR 2089). The authors are solely responsible for the content.

REFERENCES

ABAQUS, 2011. ABAQUS Analysis User's Manual 6.11. Dassault Systemes Simulia Corp., Providence.

Chae, S., 2006. Nonlinear Finite Element Modeling and Analysis of a Truck Tire. The Pennsylvania State University, University Park.

Continental, 2017. Technical Databook. Available at: https://www.conti.nl/wp-content/uploads/2014/10/Technical-Databook-car-4x4-van-2014-2015-EN.pdf. (Accessed 1 February 2017).

FGSV, 2009. Instructions for Determining the Stiffness and Fatigue Performance of Asphalt with the Dynamic Indirect Tensile Test as an Input Variable in the Dimensioning. AL Sp-09 Asphalt. FGSV Publisher, Research Society for Road and Transportation, Cologne.

Gohl, S., 2006. Vergleich der gemessenen mechanischen Beanspruchungen der Modellstraße der BASt mit den Berechnungsergebnissen ausgewählter Programme (Master thesis). Universität Dresden, Dresden.

Gonzalez, B.J., Oeser, V., 2012. Development of a Nonlinear Finite Element Pavement Response to Load Model. No. AP-T199-12. Austroads Publication, Sydney.

Hu, J., Liu, P., Wang, D., et al., 2016. Investigation on fatigue damage of asphalt mixture with different air-voids using microstructural analysis. Construction and Building Materials 125, 936–945.

Kaliske, M., Wollny, I., Behnke, R., et al., 2015. Holistic analysis of the coupled vehicle-tire-pavement system for the design of durable pavements. Tire Science and Technology 43 (2), 86–116.

Krause, G., Maerschalk, G., 2010. Auswertung von forschungsarbeiten zur weiterentwicklung des pavement management systems (PMS). In: Schriftreihe Straßenbau und Straßenverkehrstechnik. Bundesministerium für verkehrs and Uigitale Infrastruktur, Bonn, 2010.

Lin, Y.J., Hwang, S.J., 2004. Temperature prediction of rolling tires by computer simulation. Mathematics and Computer in Simulation 67 (3), 235–249.

Liu, P., Hu, J., Wang, D., et al., 2017a. Modelling and evaluation of aggregate morphology on asphalt compression behavior. Construction and Building Materials 133, 196–208.

Liu, P., Otto, F., Wang, D., et al., 2017b. Measurement and evaluation on deterioration of asphalt pavements by geophones. Measurement 109, 223–232.

Liu, P., Wang, D., Hu, J., et al., 2017c. SAFEM – software with graphical user interface for fast and accurate finite element analysis of asphalt pavements. Journal of Testing and Evaluation 45 (4), 1301–1315.

Liu, P., Wang, D., Oeser, M., 2013. Leistungsfähige semi-analytische Methoden zur Berechnung von Asphaltbefestigungen. In: Dresdner Asphalttage, Dresten, 2013.

Liu, P., Wang, D., Oeser, M., 2015. Application of semi-analytical finite element method coupled with infinite element for analysis of asphalt pavement structural response. Journal of Traffic and Transportation Engineering (English Edition) 2 (1), 48–58.

Liu, P., Wang, D., Oeser, M., 2017d. Application of semi-analytical finite element method to analyze asphalt pavement response under heavy traffic loads. Journal of Traffic and Transportation Engineering (English Edition) 4 (2), 206–214.

Liu, P., Wang, D., Oeser, M., et al., 2014. Einsatz der semi-analytischen finite-elemente-methode zur beanspruchungszustände von asphaltbefestigungen. Bauingenieur 89 (7/8), 333–339.

Liu, P., Wang, D., Otto, F., et al., 2016. Application of semi-analytical finite element method to evaluate asphalt pavement bearing capacity. International Journal of Pavement Engineering 19 (6), 1–10.

Oeser, M., Möller, B., 2002. FE-be Computational Model for Multi-layered Road Constructions, 3D Finite Element for Pavement Analysis. Design and Research, Amsterdam.

Panhead and Flathead Documentation, 2017. Tire Sizing Diagram. Available at: http://www.hydra-glide.com/joomla/index.php/documentation/miscellaneous/473-tire-sizing-diagram. (Accessed 1 February 2017).

Rabe, R., 2004. Bau einer instrumentierten Modellstraße in Asphaltbauweise zur Messtechnischen Erfassung der Beanspruchungssituation im Straßenaufbau. Bundesanstalt für Straßenwesen, Bergisch Gladbach.

Rabe, R., 2007. Messtechnische Erfassung der Beanspruchungen im Straßenaufbau Infolge LKW-Überfahrten über eine Modellstraße in Asphaltbauweise. Bundesanstalt für Straßenwesen, Bergisch Gladbach.

Rabe, R., 2014. Angaben zum Aufbau der Modellstraße und Angabe von ausgewählten Ergebnissen und Materialkennwerten. Bundesanstalt für Straßenwesen, Bergisch Gladbach.

Song, Y., 2005. Study of relationship between road surface evenness and ride quality. Road Machinery and Construction Mechanization 12, 18–21.

Ueckermann, A., Steinauer, B., 2008. The weighted longitudinal profile. Road Materials and Pavement Design 9 (2), 135–157.

Ueckermann, A., Wang, D., Oeser, M., Steinauer, B., 2015. Calculation of skid resistance from texture measurements. Journal of Traffic and Transportation Engineering (English Edition) 2 (1), 3–16.

Wang, H., Al-Qadi, I.L., Stanciulescu, I., 2012. Simulation of tire-pavement interaction for predicting contact stresses at static and various rolling conditions. International Journal of Pavement Engineering 13 (4), 310–321.

Wang, D., Liu, P., Wang, H., et al., 2017a. Modeling and testing of road surface aggregate wearing behaviour. Construction and Building Materials 131, 129–137.

Wang, H., Wang, D., Liu, P., et al., 2017b. Development of morphological properties of road surfacing aggregates during the polishing process. International Journal of Pavement Engineering 18 (4), 367–380.

Wollny, I., Behnke, R., Villaret, K., et al., 2016a. Numerical modelling of tyre–pavement interaction phenomena: coupled structural investigations. Road Materials and Pavement Design 17 (3), 563–578.

Wollny, I., Hartung, F., Kaliske, M., 2016b. Numerical modeling of inelastic structures at loading of steady state rolling. Computational Mechanics 57 (5), 867–886.

Wollny, I., Kaliske, M., 2013. Numerical simulation of pavement structures with inelastic material behaviour under rolling tyres based on an arbitrary Lagrangian Eulerian (ALE) formulation. Road Materials and Pavement Design 14 (1), 71–89.

Yao, Z., 2006. Highway Design Manual Pavement. China Communications Press, Beijing.

Zhang, J., Wang, M., Wang, D., et al., 2017. Feasibility study on measurement of a physiological index value with an electrocardiogram tester to evaluate the pavement evenness and driving comfort. Measurement 117, 1–7.

Zienkiewicz, O.C., Taylor, R.L., 2000. The Finite Element Method Volume 1. The Basis Elsevier Butterworth-Heinemann, Oxford.

Zienkiewicz, O.C., Taylor, R.L., 2005. The Finite Element Method for Solid and Structural Mechanics, sixth ed. The Basis Elsevier Butterworth-Heinemann, Oxford.

Zopf, C., Wollny, I., Kaliske, M., et al., 2015. Numerical modelling of tyre–pavement-interaction phenomena: constitutive description of asphalt behaviour based on triaxial material tests. Road Materials and Pavement Design 16 (1), 133–153.

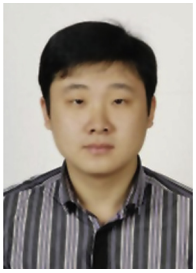

Dr. Pengfei Liu is a senior research engineer in Institute of Highway Engineering in RWTH Aachen University, Germany. His main research areas could be summarized as pavement engineering, numerical methods applied in asphalt pavement, microstructural modeling and characterization of asphalt mixtures. His work has been published in about 30 peer reviewed SCI indexed journal papers.

M.Sc. Visaagan Ravee obtained his master's degree from RWTH Aachen University in 2017. He completed his master thesis at Institute of Highway Engineering in Aachen, Germany under the supervision of Univ. Prof. Dr.-Ing. habil. Markus Oeser, Prof. Dr.-Ing. Dawei Wang and Dr. Pengfei Liu. His main area of interest is product development for transfer systems, FEM modeling and python programming.

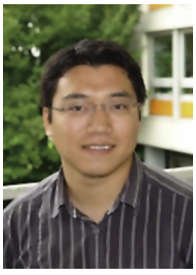

Prof. Dr.-Ing. Dawei Wang's main areas of experiences could be summarized as pavement engineering, statistics and mineralogy and focusing on aspects such as porous asphalt, reuse of engineering materials, advanced modeling and characterization of recycled engineering materials, skid resistance and traffic noise reduction. His work has been published in about 80 peer reviewed journal papers including the International Journal of Pavement Engineering, Transportation Research Record, Construction and Building Materials, Wear, and others.

Prof. Dr.-Ing. habil. Markus Oeser is the chair-professor of pavement engineering, the director of the Institute for Pavement Engineering and the dean of Faculty of Civil Engineering at the RWTH Aachen University, Germany. His research and teaching mainly focus on numerical methods (FEM, FSAFEM, BEM), constitutive models (elsto-visco-plastic models, hypo-elastic models, critical state concept) and so on. He is an active member at the International Conference on Asphalt Pavements. His work has been published in more than 70 peer reviewed journal papers.